

**SUPPORTING INFORMATION**

**Viscoelastic Properties of Polymer-Grafted  
Nanoparticle Composites from Molecular Dynamics  
Simulations**

Gregory D. Hattemer and Gaurav Arya\*

*Department of NanoEngineering  
University of California, San Diego  
9500 Gilman Drive, Mail Code 0448  
La Jolla, CA 92093*

E-mail: [garya@ucsd.edu](mailto:garya@ucsd.edu)

Phone: 858-822-5542. Fax: 858-534-9553

---

\*To whom correspondence should be addressed

## S1. Testing for NP dispersion

Given that grafted NPs exhibit strong steric repulsion due to the grafted chains and that the bare NPs exhibit weak attraction with the matrix, we do not expect to observe significant aggregation of the NPs that would otherwise mask the effects of the parameters being investigated. To confirm that our NPs remain sufficiently dispersed, we computed the radial distribution function  $g_{\text{NP}}(r)$  of the NPs, where  $r$  is the center-to-center distance between the NPs. We find that none of the systems exhibit any significant peaks in  $g_{\text{NP}}(r)$ , suggesting that the systems remain reasonably well dispersed. Figure S1 presents  $g_{\text{NP}}(r)$  of three of our NP systems most prone to aggregation, which are all observed to exhibit moderate peaks of height  $< 1.5$ . The thumb rules proposed by Kumar et al.,<sup>1</sup> based on calculation of an effective grafting density  $\Gamma_{\text{graft}}\sqrt{L_{\text{graft}}}$  and the ratio of the matrix to graft chain length  $L_{\text{matrix}}/L_{\text{graft}}$ , also suggest that all our grafted NPs systems should remain reasonably well dispersed in the polymer matrix. While these rules predict the bare NPs to aggregate, we do not observe any such aggregation, likely due to the weak attraction present between the NP surfaces and the matrix chains.

## S2. Testing for sampling exhaustiveness.

The PNC systems simulated here are expected to exhibit sluggish dynamics in spite of  $T > T_g$ .<sup>2</sup> To test if our simulations are sufficiently long to capture the equilibrium dynamics of the PNCs, we have computed the self-diffusion coefficient  $D_s$  and the rotational relaxation time  $\tau_{\text{rot}}$  of the NPs and of the matrix chains. Table S2 reports the computed  $D_s$  and  $\tau_{\text{rot}}$  of NPs for all systems studied; the results for the matrix chains are not reported as their diffusional and rotational timescales are consistently smaller than or equivalent to those of the NPs. We find that the characteristic time  $\tau_{\text{diff}} \sim d_{\text{NP}}^2/6D_s$  for the NPs to diffuse a distance equivalent to their diameter is on the order of  $10^4$ , which is smaller or comparable to the length of the MD equilibration period and significantly smaller than the length of an entire simulation. The rotational timescales  $\tau_{\text{rot}}$ , however, are longer, in the range  $10^4$ – $10^5$  for most systems investigated here, i.e., longer than the equilibration period but still much shorter than the overall simulation lengths. The only exceptions are the system with long grafts with  $L = 40$ , where  $\tau_{\text{rot}} \approx 2 \times 10^5$  is comparable to the overall simulation length, and the system with strongly attractive graft/matrix interactions, where  $\tau_{\text{rot}} \approx 1.2 \times 10^6$  is significantly longer than the simulation length. That the rotational relaxation time of grafted NPs can be quite long has already been noted in one study.<sup>2</sup> The above calculations indicate that our simulations should be able to fully capture the entire stress relaxation spectrum for most of the examined PNC systems except the system with strongly attractive interactions, which would require prohibitively long simulations.

## S3. Energetics of introducing an additional attractive site.

To estimate the enthalpic and entropic changes associated with the introduction of an additional attractive bead on the matrix and grafted chains, we have computed the radial distribution function  $g(r)$  between the mutually attractive beads on the grafted and matrix chains. For the moderately attractive system with  $n_{\text{att}} = 1$  attractive bead at the free end of

each grafted chain and  $n_{\text{att}} = 1$  attractive bead in the middle and end of each matrix chain, we compute  $g(r)$  between the centers of the mutually attractive beads on the grafted and matrix chains. For the strongly attractive system, where there are  $n_{\text{att}} = 2$  attractive beads at the free end of each grafted chain and  $n_{\text{att}} = 2$  consecutive attractive beads in the middle and end of each matrix chain, we compute  $g(r)$  between the midpoints of pairs of mutually attractive beads on the grafted and matrix chains. Figure S4 shows the two  $g(r)$  alongside each other.

One can provide a rough estimate of the difference in the binding free energy  $\Delta G_b$  of mutually attractive beads in the two systems via  $\Delta G_b = -k_B T \ln[P_{b,2}/P_{b,1}]$ , where  $P_{b,1}$  and  $P_{b,2}$  are the probabilities of observing a “bound state” in the moderately and strongly attractive case, given simply by the number of bound states in the simulation box divided by the total number of attractive bead sites in the simulation box, i.e, number of attractive beads when  $n_{\text{att}} = 1$  and number of midpoints of consecutive attractive beads when  $n_{\text{att}} = 2$ . It can easily be shown that  $P_{b,i}$  ( $i = 1, 2$ ) is given by the volume integral over the peaks in  $g(r)$  observed at sufficiently short distances divided by the volume  $V$  of the simulation box:

$$P_{b,i} \sim \frac{1}{V} \int_0^{r_{\text{cut}}} 4\pi r^2 g(r) dr, \text{ where } i = 1, 2 \quad (1)$$

where  $r_{\text{cut}}$  is the cutoff distance defining the bound state, assigned as the distance at which the peak in  $g(r)$  levels off ( $r_{\text{cut}} = 1.65$  for  $n_{\text{att}} = 1$  and  $r_{\text{cut}} = 3.65$  for  $n_{\text{att}} = 2$ ). Carrying out the above integral for both systems, we obtain  $\Delta G_b \approx -2.2k_B T$ . The maximum potential energy (enthalpy) that can be gained from adding an additional pair of mutually attractive beads should equal the depth of the attractive potential well, which is set to  $\phi = -2.5k_B T$  in our model. Thus, the enthalpic gain can be as large as  $-2.5k_B T$  whereas the entropic loss is as small as  $\sim 0.3k_B T$ , leading to a net binding free energy gain of  $-2.2k_B T$ . Thus, the enthalpic gain far outweighs the entropic loss when one introduces an additional attractive bead next to an existing attractive bead in the grafted and matrix chains.

Table S1: Radius of gyration of the grafted chains and normalized grafting density.<sup>a</sup>

System no. <sup>b</sup>	Parameter change <sup>c</sup>	$R_g^d$	$R_{g,b}^e$	$\Gamma^{*f}$
	B/G	NP grafting		
1	B	NA	NA	0
2	G	1.55	2.18	1.90
3	B	NA	NA	0
4	G	1.58	2.18	1.90
5	B	NA	NA	0
6	G	1.60	2.18	1.90
	$d_{NP}$	NP size		
2	4.0	1.55	2.18	1.90
4	6.0	1.58	2.18	1.90
6	8.0	1.60	2.18	1.90
	$f_{NP}$	NP loading		
2	0.06	1.55	2.18	1.90
7	0.12	1.56	2.18	1.90
4	0.06	1.58	2.18	1.90
8	0.12	1.56	2.18	1.90
6	0.06	1.60	2.18	1.90
9	0.12	1.60	2.18	1.90
	$L_{graft}$	Graft length		
10	10	0.74	1.47	0.86
4	20	1.58	2.18	1.90
11	30	2.43	2.72	2.96
12	40	3.28	3.16	3.98
	$\Gamma_{graft}$	Graft density		
13	0.1	1.54	2.18	0.48
14	0.2	1.55	2.18	0.95
4	0.4	1.58	2.18	1.90
15	0.8	1.56	2.18	3.80
	$n_{att}$	Graft/matrix affinity		
2	0	1.55	2.18	1.90
16	1	1.62	2.18	1.90
17	2	1.76	2.18	1.90

<sup>a</sup> Radius of gyration of matrix chains  $R_g \approx 3.16$ . Statistical uncertainties in all recorded data are smaller than the last significant figure. <sup>b</sup> Index identifying different simulation system (same as Table 1) <sup>c</sup> Only the parameter being changed in the comparison group of simulation is tabulated (refer to Table 1 for the entire list of fixed parameters). <sup>d</sup> Radius of gyration of the grafted chains computed via  $R_g^2 = \frac{1}{N_{graft}} \sum_{i=1}^{N_{graft}} \langle |\mathbf{r}_i - \mathbf{r}_{com}|^2 \rangle$ , where  $\mathbf{r}_i$  is the position of each graft bead,  $\mathbf{r}_{com}$  is the center of mass of the grafted chain, and  $\langle \dots \rangle$  represents an ensemble average over all grafted chains and time points. <sup>e</sup> Radius of gyration of an “unperturbed” grafted chain, i.e., a polymer matrix chain of the same length as the grafted chain.

<sup>f</sup> Crowding of grafted chains on NPs quantified in terms of the grafting density normalized by the size of the unperturbed grafted chains, i.e.,  $\Gamma^* = R_{g,b}^2 \Gamma_{graft}$ .

Table S2: Diffusion coefficient and rotational relaxation time of NPs.

System no. <sup>a</sup>	Parameter change <sup>b</sup>	$D_s$ <sup>c</sup> ( $\times 10^3$ )	$\tau_{\text{rot}}$ <sup>d</sup> ( $\times 10^{-4}$ )
	B/G	NP grafting	
1	B	$1.52 \pm 0.39$	NA
2	G	$3.91 \pm 0.95$	$2.28 \pm 0.15$
3	B	$1.12 \pm 0.42$	NA
4	G	$2.71 \pm 0.02$	$5.54 \pm 0.44$
5	B	$0.57 \pm 0.19$	NA
6	G	$2.00 \pm 0.58$	$10.80 \pm 3.17$
	$d_{\text{NP}}$	NP size	
2	4.0	$3.91 \pm 0.95$	$2.28 \pm 0.15$
4	6.0	$2.71 \pm 0.02$	$5.54 \pm 0.44$
6	8.0	$2.00 \pm 0.58$	$10.80 \pm 3.17$
	$f_{\text{NP}}$	NP loading	
2	0.06	$3.91 \pm 0.95$	$2.28 \pm 0.15$
7	0.12	$2.72 \pm 1.69$	$2.40 \pm 0.12$
4	0.06	$2.71 \pm 0.02$	$5.54 \pm 0.44$
8	0.12	$1.27 \pm 0.57$	$6.76 \pm 0.53$
6	0.06	$2.00 \pm 0.58$	$10.80 \pm 3.17$
9	0.12	$1.31 \pm 1.07$	$12.12 \pm 1.69$
	$L_{\text{graft}}$	Graft length	
10	10	$2.84 \pm 0.67$	$2.00 \pm 0.13$
4	20	$2.71 \pm 0.02$	$5.54 \pm 0.44$
11	30	$1.74 \pm 0.09$	$15.19 \pm 1.60$
12	40	$2.89 \pm 1.98$	$20.51 \pm 0.34$
	$\Gamma_{\text{graft}}$	Graft density	
13	0.1	$1.80 \pm 0.12$	$1.63 \pm 0.14$
14	0.2	$2.03 \pm 0.55$	$3.11 \pm 0.56$
4	0.4	$2.71 \pm 0.02$	$5.54 \pm 0.75$
15	0.8	$2.12 \pm 0.73$	$10.74 \pm 1.17$
	$n_{\text{att}}$	Graft/matrix affinity	
2	0	$3.91 \pm 0.95$	$2.28 \pm 0.15$
16	1	$2.03 \pm 1.43$	$6.74 \pm 0.56$
17	2	$2.99 \pm 1.97$	$116.00 \pm 9.68$

<sup>a</sup> Index identifying different simulation system (same as Table 1) <sup>b</sup> Only the parameter being changed in the comparison group of simulation is tabulated (refer to Table 1 for the entire list of fixed parameters). <sup>c</sup>  $D_s$  was computed from the slope of the mean square displacement of the NPs as a function of time via  $D_s = \lim_{t \rightarrow \infty} \frac{1}{6t} \langle |\mathbf{r}(t) - \mathbf{r}(0)|^2 \rangle$ , where  $\mathbf{r}(t)$  is the position of NP center at time  $t$  and  $\langle \dots \rangle$  represents an ensemble average over all NPs and reference time points. <sup>d</sup>  $\tau_{\text{rot}}$  was computed by fitting the time decay in the autocorrelation of the orientation of the NPs to an exponential function via  $\langle \mathbf{T}(t) \cdot \mathbf{T}(0) \rangle \approx \exp(-t/\tau_{\text{rot}})$ , where the orientation is described in terms of the vector  $\mathbf{T}(t)$  joining one of grafting points and the NP center.

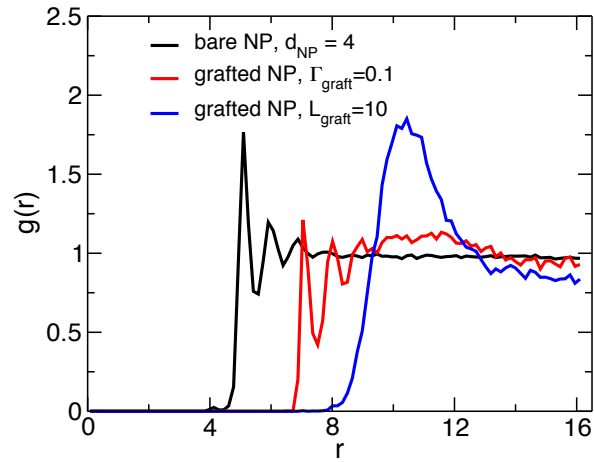


Figure S1: Inter-particle radial distribution function  $g(r)$  obtained for three PNC systems from Table 1 most prone to NP aggregation: system 7 containing bare NPs of  $d_{\text{NP}} = 4$  at the high loading of  $f_{\text{NP}} = 0.12$  (black line); system 13 containing grafted NPs of  $d_{\text{NP}} = 6$  at the small grafting density  $\Gamma_{\text{graft}} = 0.1$  (red line); and system 10 containing grafted NPs of  $d_{\text{NP}} = 6$  with short grafts of  $L_{\text{graft}} = 10$  (blue line).

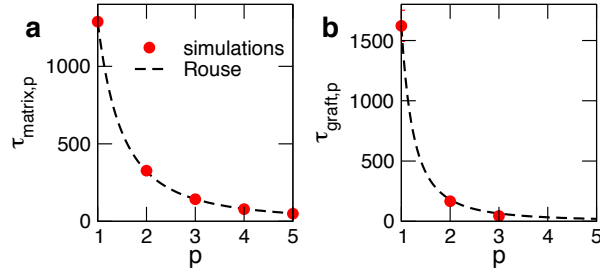


Figure S2: Relaxation times for the five slowest modes  $p$  of the matrix chains (a) and for grafted chains (b) for PNCs with grafted NPs (system 4, Table 1). The symbols represent  $\tau_{\text{matrix},p}$  and  $\tau_{\text{graft},p}$  obtained by fitting the autocorrelation of Rouse modes obtained from simulations (Eqs. 11 and 13). We were unable to obtain good estimates of the Rouse times for  $p > 3$  for the grafted chains, as these times became comparable to the smallest time intervals used for calculating Rouse modes. The dashed lines represent predictions from Rouse theory via the approximations  $\tau_{\text{matrix},p} \approx \tau_{\text{matrix},R}/p^2$  and  $\tau_{\text{graft},p} \approx \tau_{\text{graft},R}/(2p - 1)^2$  valid for small  $p$ .

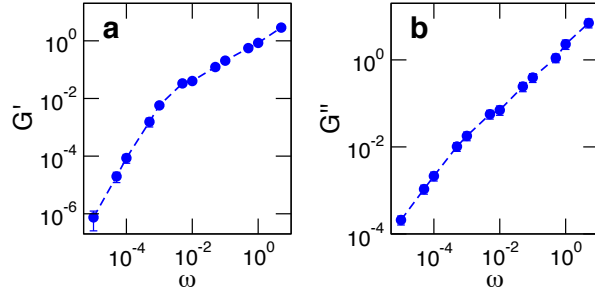


Figure S3: Storage modulus (a) and loss modulus (b) of pure polymer matrix of chain length  $L_{\text{matrix}} = 40$  at overall monomer density  $\rho_{\text{polymer}} = 0.82$  and temperature  $T = 1$ . The symbols represent computed data while dashed lines are guides to the eye.

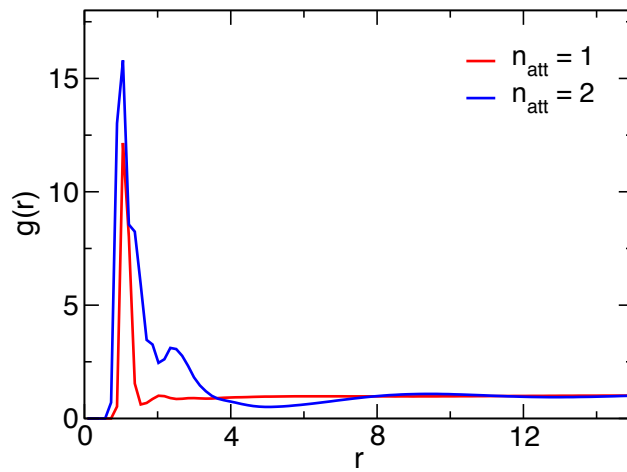


Figure S4: Radial distribution function  $g(r)$  of distance between mutually attractive beads for  $n_{\text{att}} = 1$  (red) and of distance between the midpoints of mutually attractive bead pairs for  $n_{\text{att}} = 2$  (blue).

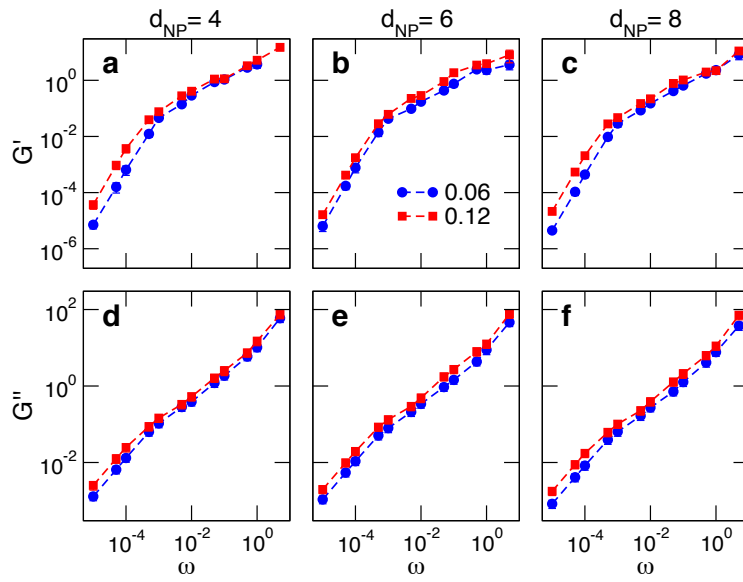


Figure S5: Comparison of the storage and loss modulus of polymers containing grafted NPs at two different loadings of  $f_{NP} = 0.06$  (blue circles) and  $0.12$  (red squares) for (a)  $d_{NP} = 4$ , (b)  $d_{NP} = 6$ , and (c)  $d_{NP} = 8$ . The symbols represent computed data while dashed lines are guides to the eye.

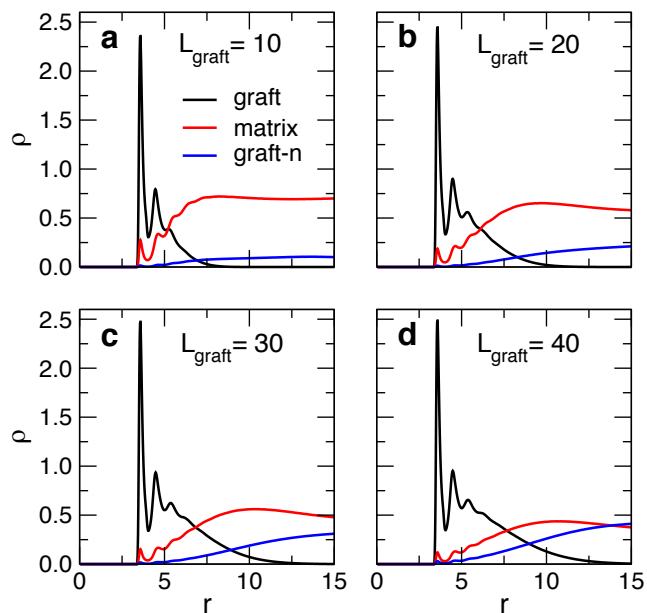


Figure S6: Comparison of monomer densities of four different PNCs containing NPs grafted with chains of different lengths: (a)  $L_{\text{graft}} = 10$ , (b)  $L_{\text{graft}} = 20$ , (c)  $L_{\text{graft}} = 30$ , and (d)  $L_{\text{graft}} = 40$ . The NPs have a diameter of  $d_{\text{NP}} = 6$  and are loaded at  $f_{\text{NP}} = 6$  wt% ( $\phi_{\text{NP}} = 0.027$ ) in a polymer matrix of chain length  $L_{\text{matrix}} = 40$ . The densities are plotted as a function of the radial distance from the center of a NP and the contributions from grafted chains, matrix chains, and grafted chains on neighboring NPs plotted as solid black, red, and blue lines, respectively.

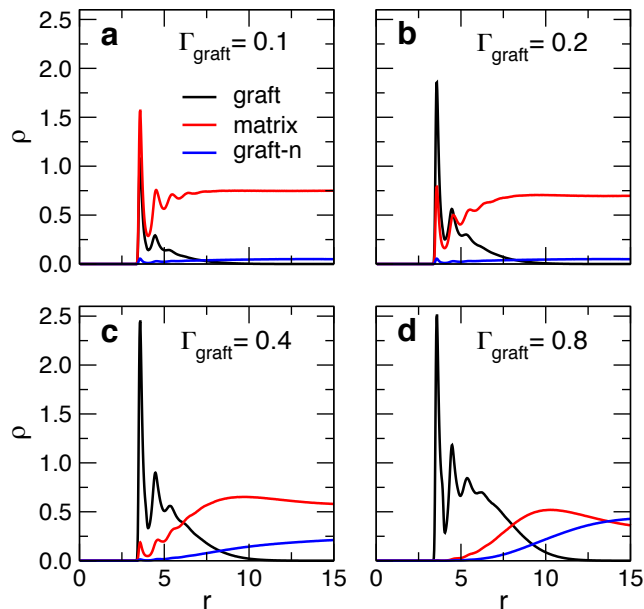


Figure S7: Comparison of monomer densities of four PNC systems containing NPs grafted with chains at different grafting densities: (a)  $\Gamma_{\text{graft}} = 0.1$ , (b)  $\Gamma_{\text{graft}} = 0.2$ , (c)  $\Gamma_{\text{graft}} = 0.4$ , and (d)  $\Gamma_{\text{graft}} = 0.8$ . The NPs have a diameter of  $d_{\text{NP}} = 6$  and are loaded at  $f_{\text{NP}} = 6$  wt% ( $\phi_{\text{NP}} = 0.027$ ) in a polymer matrix of chain length  $L_{\text{matrix}} = 40$ . The densities are plotted as a function of the radial distance from the center of a NP and the contributions from grafted chains, matrix chains, and grafted chains on neighboring NPs plotted as solid black, red, and blue lines, respectively.

## References

- (1) Kumar, S. K.; Jouault, N.; Benicewicz, B.; Neely, T. *Macromolecules* **2013**, *46*, 3199–3214.
- (2) Meng, D.; Kumar, S. K.; Lane, J. M. D.; Grest, G. S. *Soft Matter* **2012**, *8*, 5002–5010.